Supplementary Figure 1 **Wu** *et al.*

(A) 128 representative class averages of native RNAPII(G) obtained after reference-free alignment and CL2D clustering from ~7689 particles. (B) Resolution assessment of native RNAPII(G) EM reconstructions. The Fourier shell correlation (FSC) is shown in orange. (C) Immuno analysis of RNAPII dimer interaction. Antibody against the Rpb3, Rpb2 and Rpb5 subunits were individually incubated with RNAPII and preserved in negative stain (2% uranyl acetate). Percentages of monomer from EM photos were calculated.

A

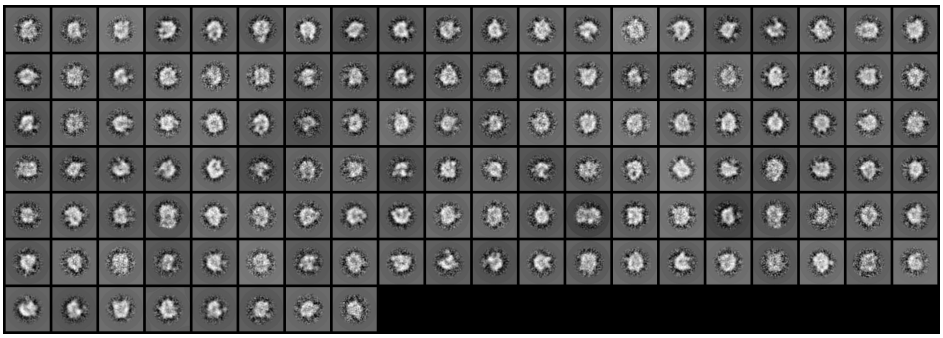

B

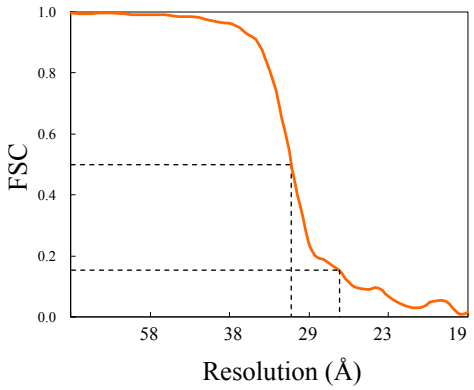

C

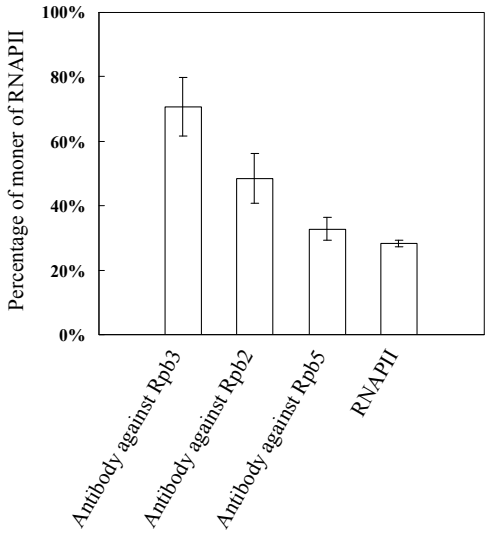

Supplementary Figure 2 **Wu** *et al.*

Single particle analysis of bovine RNAP II elongation complexes. (A) Sequence of the DNA/RNA scaffold. (B) Cryo electron micrograph of bovine RNAP II with the DNA/RNA scaffold. The bars correspond to 50 nm. (C) EM reconstruction of cryo-stained bovine RNAPII elongation complex compared with the X-ray structure of yeast RNAPII (colored ribbons) (PDB: 1Y1W). (D) Flow chart of EM reconstruction process in this study.

A

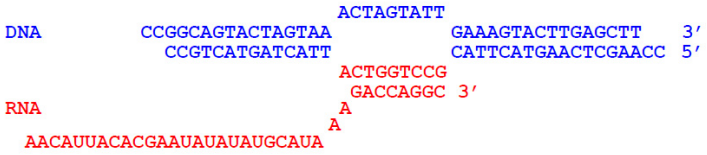

B

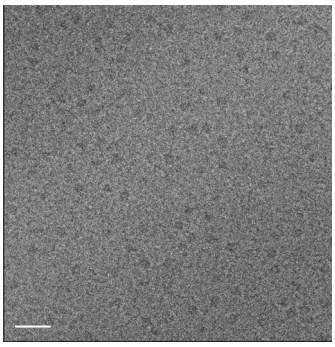

C

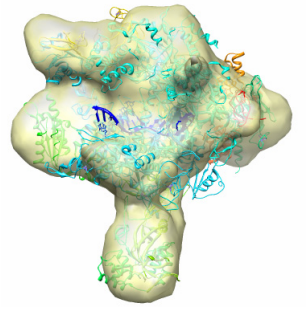

D

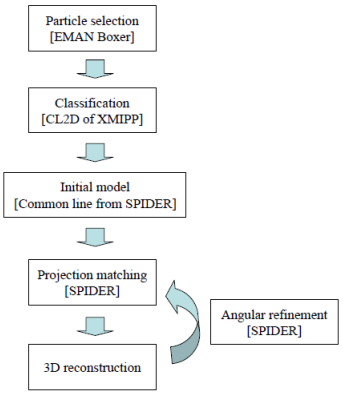

Supplementary Figure 3 Wu *et al.*

Analysis of bovine RNAPII-rGdown1. (A) Purification of recombinant Gdown1 protein. (B) Cryo electron micrograph of bovine RNAP II-rGdown1. The bars correspond to 50 nm. (C) Left, a positive difference map was calculated between the bovine RNAPII-Gdown1 and bovine RNAPII elongation complex (gray mesh) shown in green hue above 5 σ. The most conspicuous density above 10 σ is in the gap between the Rpb5 shelf and the Rpb1 jaw is shown in deep green. Right, a negative difference map was shown in red hue. The additional densities attributed to the RNAPII elongation complex are likely to the result of conformational changes (outer densities) and nucleic acids (internal 10 σ densities in the cleft and active site). (D) A positive difference map between the bovine RNAPII-Gdown1 elongation and bovine RNAPII elongation complex showed that the density ascribed to Gdown1 was detected on Rpb3 (red ribbon). (E) Resolution assessment of bovine RNAP II-rGdown1 elongation and RNAPII-rGdown1 reconstructions. The FSC of is shown in orange and blue, respectively. (F) Pull down assays of rGdown1 and rRpb5 on SDS-PAGE. Lane 1: GST-rGdown1, Lane 2: His-Rpb5, Lane 4-7: Mixture of GST-Gdown1/His-Rpb5 passed though Ni-NTA then GST column.

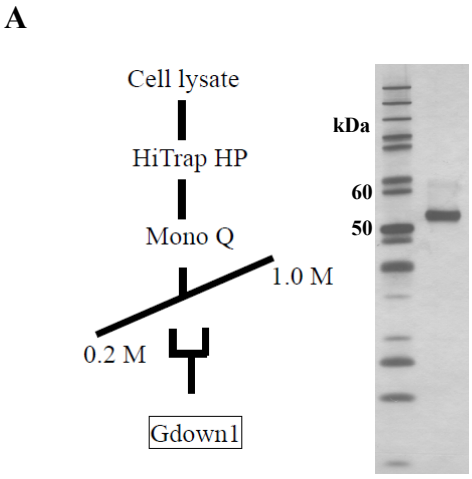
A
Cell lysate
HiTrap HP
Mono Q
1.0 M
0.2 M
Gdown1
kDa
60
50

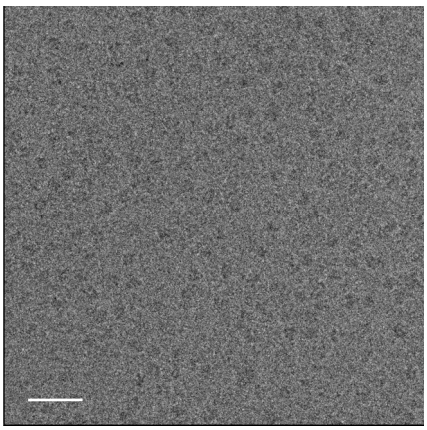
B

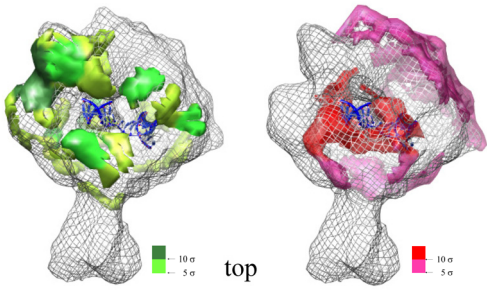
C
top

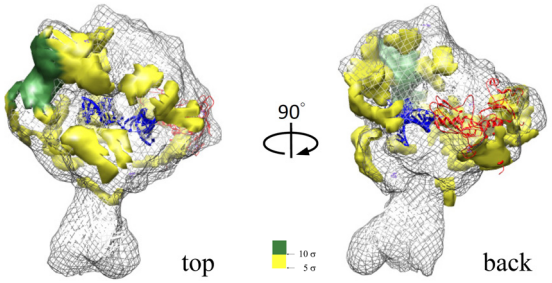
D
top
90°
back

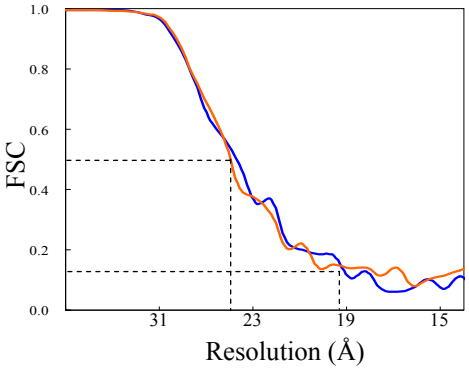
E
FSC
Resolution (Å)
1.0
0.8
0.6
0.4
0.2
0.0
31
23
19
15

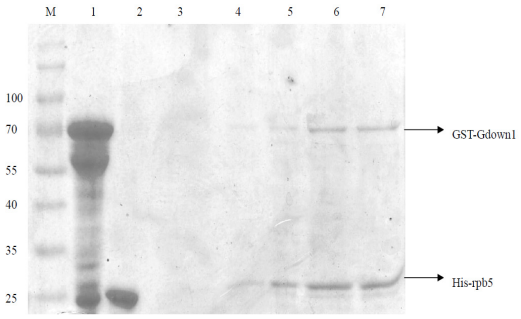
F
M
1
2
3
4
5
6
7
100
70
55
40
35
25
GST-Gdown1
His-rpb5

Supplementary Figure 4

Single particle analysis of bovine RNAP II-TFIIF. **(A)** Purification of recombinant human TFIIF protein. **(B)** Cryo electron micrograph of bovine RNAP II-TFIIF. The bars correspond to 50 nm. **(C)** Folding analysis of TFIIF. The result shows that there is a very small domain (green regions) in native state RAP74. By contrast, RAP30 has two major folded domains. **(D)** Resolution assessment of EM reconstructions. The FSC is shown in orange.